PLLA porous scaffold as a 3D breast cancer model to investigate drug resistance

Camilla Carbone[a], Salvatrice Rigogliuso[b*], Valerio Maria Bartolo Brucato[a], Alessandra Cusimano[b], Manuela Labbozzetta[b], Vincenzo La Carrubba[a], Paola Poma[b], Monica Notarbartolo [b], Francesco Carfì Pavia[a]

[a]Engineering Department, University of Palermo, Viale delle Scienze building 6, Palermo, Italy.

[b]Department of Biological, Chemical, and Pharmaceutical Sciences and Technologies (STEBICEF), University of Palermo, Viale delle Scienze building 16, Palermo, Italy.

*salvatrice.rigogliuso@unipa.it

1 Abstract

Multidrug resistance remains one of the major challenges in breast cancer research leading to treatment failure. To better understand this mechanism new sophisticated three-dimensional (3D) tumor model are necessary cause they offer several advantages over traditional bidimensional cultures (2D). In this study Poly-L-Lactic-Acid porous scaffold have been produced via Thermally Induced Phase Separation technique and employed as three-dimensional model for breast cancer cell lines: MDA-MB-231, MCF-7 and its multidrug resistant variant MCF-7R. MTS assay was used to compare growth inhibition after doxorubicin treatment in 2D and in 3D. Remarkably the IC_{50} values increased in 3D cultures compared to 2D: MDA-MB-231 (445 ng/ml vs. 54.5 ng/ml), MCF-7 (7.45 μg/ml vs. 0.75 μg/ml), and MCF-7R (165 μg/ml vs. 39 μg/ml). Remarkably MCF-7R, that usually displays greater resistance in 2D, showed even higher resistance in 3D: in fact, IC_{50} was not reached within 3 days as the other models, but only at 6 days. Cellular morphology played a crucial role too. In fact, when treated with a concentration higher then $IC_{50,}$ MDA-MB-231 lost their physiological 3D clustered structure while MCF-7 and its resistant variant exhibited disrupted layers. All cell lines in 3D displayed higher chemoresistance suggesting a more biomimetic spatial architecture. Our work bridges the gap between monolayer models and animal models, highlighting the potential of polymeric 3D scaffolds in breast cancer research.

2 Introduction

Breast cancer (BC) is the most common malignant tumor in women in the world and breast cancer patients account for as much as 36% of oncological patients [1]. Over 2.3 million new cases and 685,000 deaths from breast cancer occurred in 2020 and, by 2040, the burden from breast cancer is predicted to increase to over 3 million new cases and 1 million deaths

every year [2]. In 2019, in Italy, 53,000 new cases of breast cancer have been reported, representing the most diagnosed cancer in women: it can be estimated that about one in three cancer cases in women is represented by breast cancer [3]. Finding an efficient treatment method for cancer is not easy, since it is a complex set of diseases, with patient-to-patient variance and heterogeneity between cells within the tumor [4].

One of the main problems in cancer research is the development of the resistance to chemotherapy treatments, which inevitably leads to therapy failure. The multidrug resistance (MDR) consists in the resistance of tumor cells to different drugs with multiple chemical structures, multiple mechanisms of action and multiple targets and, ultimately, these mechanisms mean that, in the tumor cell, the intracellular concentration of chemotherapeutic, effective from a therapeutic point of view, is never achieved. The development of multidrug resistance is a complex process involving several factors, often due to the genetic instability characteristic of the different cells of the tumor mass. Among these, the increase in DNA repair mechanisms, the epithelial-mesenchymal transition, the inhibition of apoptotic processes, the increase in the levels of detoxifying enzymes, and alterations of drug targets [5], [6]. Moreover, the MDR phenotype is often linked to the over-expression of MDR1 gene encoding for P-gp efflux pumps [7]. Unfortunately, the mechanisms implicated are not yet fully understood, and MDR represents one of the main causes of cancer recurrence and metastasis [8]. In recent decades, significant progress has been made in exploring the mechanisms of MDR, which has led to a growing interest in developing therapeutic strategies to overcome MDR and improve the intracellular bioavailability of the chemotherapeutic agent. Thus, it is necessary to create advanced tumor models to better understand cancer microenvironment and try to find new therapies. Breast cancer has been widely studied using different models: *in vivo, in vitro* and *in silico* [9], [10], [11].

Research is facilitated by animal models, which are very important in studying the genesis of a tumor from different perspectives [12]. These models have been crucial in giving us important insights into the intricate nature of cancer, leading to many advancements in the field [13], [14]. However, using animals raises significant ethical concerns [15], [16]. Animal models cannot fully capture the diversity of human breast cancer, which is a major limitation. Additionally, the cost, validity of results, and poor research practices are further disadvantages [16]. Ethical issues revolve around the welfare of the animals used, as there is growing awareness of animal rights; while animal models contribute to medical research, it's crucial to address these ethical issues and limitations [17], [18].

The scientific community has progressively recognized these issues, leading to an increasing study and use of *in vitro* models that are more ethical, less expensive, and allow for more controlled and reproducible experiments [19], [20]. In 2D culture models, cells are maintained in specially designed culture media, adhered to glass or plastic surfaces. Despite their widespread use, these models often fail to replicate the interactions between cellular and extracellular environments [21], [22]. They also lead to changes in cell morphology, polarity, division mechanism, differentiation, and cell motion. Moreover, 2D culture models cannot accurately mimic complex aspects of tumor cells and drug responses. As a result, they often provide less appropriate mimicry of the biological behavior of tumor cells, particularly the mechanisms leading to therapeutic escape and drug resistance [23], [24]. These limitations of 2D culture models have led to the development and adoption of more advanced *in vitro* methodologies, such as 3D cell culture models [25].

3D *in vitro* models are a promising option to overcome animal models since they present key advantages for biomedical research and drug development [26], [27]. These 3D models mimic human tumor microenvironment better than 2D cell cultures, therefore they give a more realistic way to study disease processes and drug effects, they provide a system that is very close to *in vivo* pathophysiological conditions leading to an excellent alternative to the animal model.

These models have revolutionized cancer immunology with their ability to provide more accurate data on cell-cell and cell-matrix interactions, tumor characteristic and drug response [28], [29]. In fact, they are changing how new drugs are discovered and tested in the field of breast cancer research too [30], [31].

3D models are able resemble the complex microenvironment of tissues accurately while conventional 2D cell cultures fall short in representing this complexity [32]. They are cost effective and highly reproducible, and it is possible to include human cancer and immune cells with growth factors and biomolecules [33], [34].

Several 3D systems have been used in recent years in drugs research for breast cancer. Each has special benefits and limitations. The growth of 3D printing, for example, allowed researchers to make complex support frames [35]. These supports can be geometrically complex, and this allows to study tumors growing and their response to treatment in a more physiological environment [36]. The choice of the material remains a challenge with the aim to balance mechanical properties and cytotoxicity.

Another category among 3D models are hydrogels which are rising among 3D structures often used in cancer studies [37], [38]. They are networks of linked polymers that absorb water, with tunable mechanical features, furthermore they can store growth factors and signaling molecules acting like the changing tumor surroundings [39]. Breast cancer cells can be seeded inside hydrogel structures to examine tumor behaviors in a controlled setting like invasion, angiogenesis, and resistance to drugs [40]. However, the cytocompatibility and cross-linking balance needs to be improved as solvents, UV light and free radical may be damaging to cells [41].

Polymeric porous scaffolds have become essential in this field. They are made from biocompatible polymers, natural or synthetic, with a porous architecture that mimics the intricate Extracellular Matrix (ECM) architecture of breast cancer tissue. They offer tunable properties such as pore size and stiffness, or other crucial characteristic for cell adhesion, migration, and response to drugs. Polymeric porous scaffolds provide a controlled and reproducible platform, advancing our understanding of breast cancer promoting the development of effective treatments [32].

In this study Poly-L-Lactic-Acid (PLLA) porous scaffolds were produced by Thermally Induced Phase Separation (TIPS) technique and were used as a 3D model to establish three distinct breast cancer cell lines: triple-negative breast cancer (MDA-MB-231), ER+ adenocarcinoma (MCF-7) and its multidrug-resistant variant (MCF-7R). PLLA was chosen because it is an FDA approved polymer for biomedical applications, it has been already widely used in several works. On the other hand this kind of polymers are preferable respect to hydrogels to become a 3D model for preclinical tests because they have an higher degradation time. By cultivating these cell lines on PLLA scaffolds, we aimed to create an *in vitro* microenvironment closely resembling physiological tumor conditions, enabling us to assess their response to doxorubicin, a commonly used chemotherapeutic agent. This work seeks to bridge the gap between traditional monolayer cell cultures and *in vivo* models,

highlighting the potential of 3D cultures in studying the complex interplay between cellular architecture, drug response, and molecular mechanisms in breast cancer.

3 Materials and methods

3.1 Scaffold production and characterization

Scaffolds were produced by TIPS starting from a ternary solution based on Poly-Left-Lactic Acid (PLLA, Resomer, L 209 S, Evonik Industries, Essen, Germany), 1,4-dioxane (Sigma-Aldrich, Munich, Germany) and water as described in previous work [42]. Briefly, the polymer was dissolved into 1,4 dioxane with a concentration of 4% (wt/wt). Its complete dissolution was achieved by stirring at a temperature of 180 °C for 30 minutes. Then distilled water was added dropwise with a constant dioxane to water weight ratio of 87/13 and still complete dissolution was achieved by stirring at a temperature of 180 °C. When the solution resulted homogeneous it was kept at 60°C until its usage. The solution (initially at 60°C) was poured into a High-Density Polyethylene (HDPE) cylindrical sample holder with an inner diameter of 17.6 mm and a height of 35.7 mm. The sample holder was first immersed into a thermostatic water bath (TWB) set to 20°C (demixing temperature) for a defined demixing time of 15 minutes. Subsequently, the holder was covered by a Polytetrafluoroethylene (PTFE) coating, a thermal resistance to control the cooling rate and immersed into an ethyl alcohol bath (EAB) at -20°C for at least 15 min to suddenly cool down the solution, thus preserving its porous architecture [32].

At the end of this process, cylindrical scaffolds were obtained and washed in distilled water, drop by drop overnight, to completely remove the dioxane from the inner parts of the matrix. Scaffolds were then placed at 45° C and under vacuum for 3 hours. When they were completely dry, slices of 2 mm were cut by a scalpel, from which little cylinders were extracted using a biopsy punch; these cylinder scaffolds (3,5 mm in diameter and 2 mm in height) were used for the subsequent phases.

The overall morphology of PLLA scaffolds was examined using Scanning Electron Microscopy (SEM, QUANTA 200F, FEI Company Philips, Thermo Fisher, Waltham, MA, USA) with an accelerating voltage of 10 kV. Prior to analysis, samples were cut into small slices and positioned on an aluminum stub coated with conductive carbon tabs.

Pore sizes and distribution were determined from SEM micrographs starting from a MATLAB script found in the literature made by Rabbani et al. [43]. After defining the spatial resolution and the number of intensity levels of the image segmentation, the script converts the image to a greyscale. The image is divided into multiple regions based on different intensity levels, creating a depth map and subsequently a binary segmentation. At this point the script can estimate the average pore distribution.

Porosity was evaluated through pycnometry. By measuring the change in pressure resulting from the introduction of helium, the real volume of a solid sample can be accurately determined using the principles of gas displacement. Three samples were cut starting from a big cylindrical scaffold and their apparent volumes were calculated. To completely fill the instrument chamber, the samples were inserted simultaneously into a gas pycnometer (Pycnomatic ATC, Thermo Fisher Scientific, Waltham, MA, USA) and the real volume

was determined. The porosity of the samples was determined comparing the entire real volume to the sum of apparent volumes of the scaffolds through the following equation:

$$Porosity\ \% = 1 - \left(\frac{V_{measured}}{V_{apparent}}\right) * 100$$

3.2 Cell lines and 2D culture conditions

A human breast adenocarcinoma cell line MCF-7 and a triple-negative breast cancer (TNBC) cell line MDA-MB-231 were obtained from ATCC (respectively HTB-22™ and HTB-26™, Rockville, MD, USA). MCF-7R cells were established treating wild-type cells with gradually increasing concentrations of doxorubicin (Sigma D15-15). The IC_{50} value of doxorubicin in MCF-7R is approximately 50 times higher than the original IC_{50}. Unlike MCF-7, MCF-7R lacks ERα expression, is estrogen-insensitive, and overexpresses P-gp; in addition is characterized by a constitutive activation of the NF-κB pathway, and by the overexpression of some targets of this transcription factor such as Inhibitor of Apoptosis Proteins (IAPs) which determine its resistance to drug-induced cell death. All cell lines were cultured in Dulbecco's Modified Eagle Medium (DMEM) (HyClone Europe Ltd, Cramlington, UK). All media were further supplemented with 10% heat-inactivated fetal calf serum, 2 mM L-glutamine, 100 units/ml penicillin, and 100 μg/ml streptomycin (all reagents were from HyClone Europe). All cell lines were cultured in a humidified atmosphere of 5% CO_2 at 37˚C. Cells with a narrow range of passage numbers were used for all experiments. The cultures, maintained as monolayers in complete medium, were routinely tested for Mycoplasma infection and then, when they reached the 80%-90% confluence, they were enzymatically recovered with trypsin and used in the experiments described below.

3.3 Evaluation of 3D growth on scaffolds

The scaffolds were sterilized in 70% ethanol for 8 h, washed 2 times 3 minutes each in Phosphate Buffered Saline (PBS), and soaked in Dulbecco's modified Eagle's-high glucose medium (DMEM, Sigma Aldrich, Italy) 30 min before the seeding. The seeding on scaffolds was carried out in 6-multiwell plates, one for each cell line. The samples were divided into groups of five per well to select the most suitable growth time for the experiments (24 hours, 5 days, 10 days, and 15 days); two scaffolds were used for SEM morphological analysis and three were transferred in a 96- well to perform cell viability analysis using MTS assay. The cells were seeded with a density of 4 × 10^4 cells/scaffold in 10 μL of cell suspension. Subsequently, the plates were incubated in a humidified atmosphere of 5% CO_2 at 37˚C, for one hour; finally, complete culture medium was added to fully cover the scaffolds. For each experiment, unseeded scaffolds were used as controls. At different time points, a commercial solution (MTS: Promega Corporation Madison, WI, USA) containing 3- (4,5-dimethylthiazol-2-yl) -5- (3-carboxymethoxyphenyl) - 2- (4-sulfophenyl) -2H-tetrazolium (MTS) and phenazine ethosulfate was added. The plates were incubated in a humidified atmosphere at 37°C in 5% CO_2 for 2 hours, and the bio-reduction of the MTS dye was evaluated by measuring the absorbance of each well at 490 nm using a microplate reader (iMark Microplate Reader; BioRad Laboratories, Inc., Hercules, CA, USA). MTS assay was performed in triplicate, for each chosen time point. A cell-free scaffold was used as a blank. All tests were performed in triplicate. The growth trend was expressed showing absorbance values (mean ± SE) versus the different time points.

SEM was carried out to observe cell morphologies during growth. To do so scaffolds were firstly transferred to a 96 multiwell plate and were washed with complete 1X DPBS 3 times, for 3 minutes each. Cells were fixated using 4% glutaraldehyde (Sigma Aldrich) for 30 minutes at 4 °C. Samples were rinsed with complete 1X DPBS 2 times, for 3 minutes each. Dehydration was then carried at room temperature, in solutions of ethanol at increasing concentration (15%, 30%, 50%, 75%, 100%, 3 minutes each). After the last step, the ethanol evaporated at room temperature until the samples were completely dry. Subsequently, the scaffolds were cut into two halves using a scalpel and each half was placed on the stubs with inverted faces, to be able to observe both surfaces. Finally, they were sputter coated for 120 s in argon atmosphere (Sputtering Scancoat Six, Edwards, Crawley, UK) and observed.

3.3.1 Live–Dead Assay

One milliliter of PBS containing Ca^{++} and Mg^{++} was mixed with 5 µL of fluorescein diacetate (FDA) stock solution (5 mg/mL in acetone) and 1 µL of propidium iodide (PI) stock solution (2 mg/mL in PBS). The FDA dye stains living cells in green, while the PI dye marks dead cells in red. A total of 50 µL of this staining solution was applied to each sample. Samples were observed from the outer surface and subsequently cut by a scalpel to observe the cross section, and the sample (either a seeded scaffold segment or coverslip) was immersed in it. The imaging was conducted with a fluorescent microscope (Leica DM2500) equipped with a camera (Leica DFC450 C) and LAS software Version: 4.1.0. at 1 day and 5 days.

3.4 Viability inhibition after doxorubicin treatment

For the cell proliferation assay in 2D, cell lines were seeded at 5×10^3 cells/well in 96-well plates and incubated overnight at 37°C. The medium was replaced with fresh complete medium supplemented with Doxorubicin at several concentrations. After 72 hours of treatment, 16 µl of MTS reagent was added. The plates were incubated in a humidified atmosphere at 37°C in 5% CO_2 for 2 hours, and the bioreduction of the MTS dye was evaluated by measuring the absorbance of each well at 490 nm using a microplate reader (iMark Microplate Reader; BioRad Laboratories, Inc., Hercules, CA, USA). All tests were performed in triplicate. After 5 days of 3D culture, the samples were incubated in a 96-well plate in a complete culture medium supplemented with Doxorubicin at the indicated concentrations. After 3 or 6 days of incubation, MTS assay was carried out as described before. Cell growth inhibition was expressed as a percentage (mean ± SE) of absorbance compared to control cells for MDA-MB-231, MCF-7 and MCF-7R. SEM morphological analysis was carried out as described before.

3.5 Realtime PCR

Gene expression was evaluated on cell lines MCF-7 and MCF-7R seeded on PLLA scaffold. Total cellular RNA was isolated after their lysis using a TRIzol reagent (Invitrogen Life Technologies, Carlsbad, CA, USA). For each sample, the same amount of total RNA (500 ng) was reverse-transcribed using a High-Capacity cDNA Reverse

Transcription Kit (Applied Biosystems, USA) following the protocol provided by the manufacturer. BrightGreen 2X qPCR MasterMix (Applied Biological Materials Inc. Richmond, BC V6V 2J5 Canada) was employed to analyze the obtained cDNA for quantitative real-time PCR (qRT-PCR) in triplicates. The qRT-PCR was performed using the primers: β-ActinF CGGGAAATCGTGCGTGACAT and β-ActinR GGACTCCATGCCCAGGAAGG; P-glycoproteinF GCCTGGCAGCTGGAAGACAAATACACAAAATT and P-glycoproteinR CAGACAGCAGCTGACAGTCCAAGAACAGGACT. The running of the samples and data collection were performed on a StepOne AB Real Time PCR system (Applied Biosystems Life Technologies Inc., Foster City, CA, USA). β-Actin was used as an internal standard.

3.6 Statistical analysis

The results obtained are reported as mean ± standard error (SE). Statistical analysis was performed by analysis of variance (one-way ANOVA) followed by Tukey's test. STATISTICS ver. 10 (StatSoft Inc. 2011) was used as the analysis software.

4 Results

4.1 Scaffolds morphology and porosity

As can be noticed in Figs. 1(A-C) SEM micrographs revealed a porous structure characterized by interconnected pores, essential for ensuring adequate nutrition supply, cell migration, and matrix colonization.

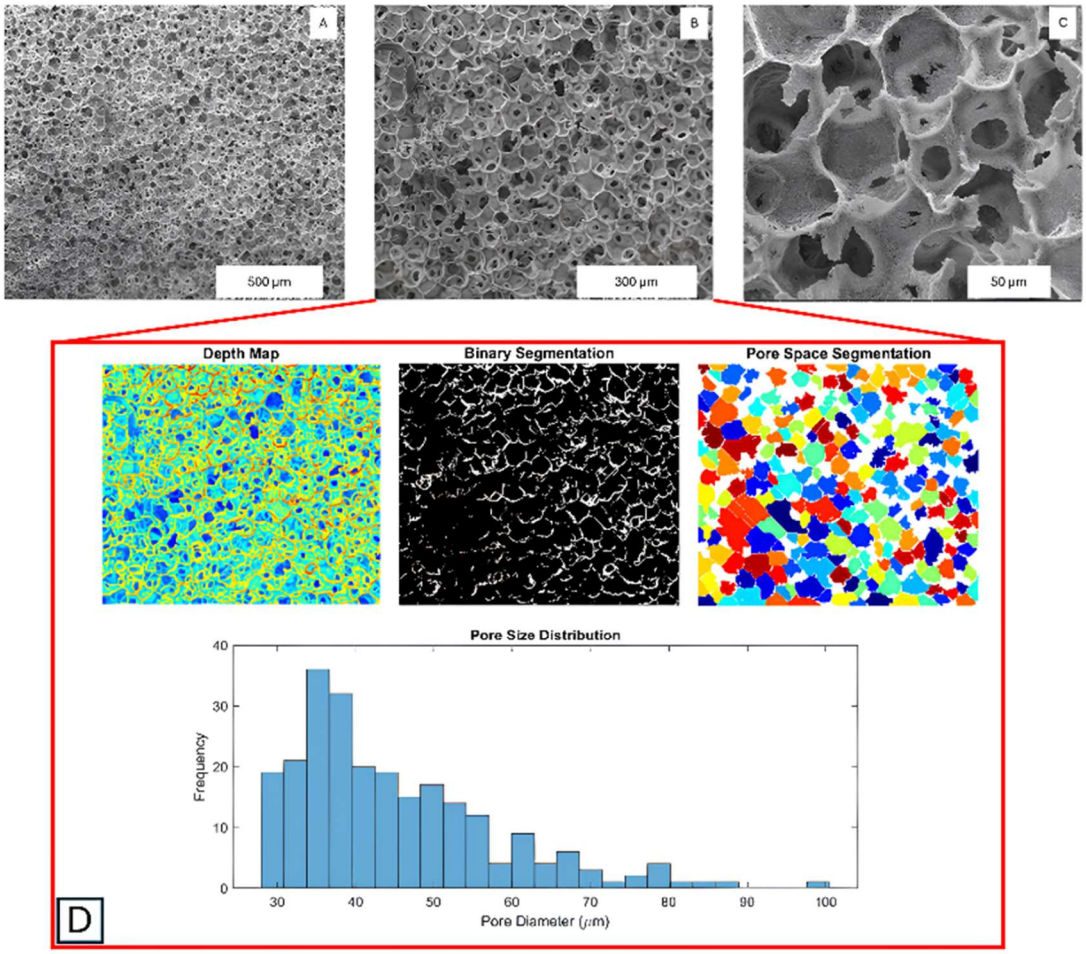

Figure 1: A, B and C Morphological characterization by SEM of the porous 3D scaffolds (TIPS parameter 20°C 15 min TWB and -20°C 15 min EAB. A) Magnification 150x, scale bar 500 µm. B) Magnification 300x, scale bar 300 µm C) Magnification 1200x scale bar 50 µm D) MATLAB results: depth map, binary segmentation, pore space segmentation and pore size distribution in micrometers

As shown in figure 1D the MATLAB code provides a depth map, a binary segmentation, and a colored pore space segmentation from which it can be extracted the pore sizes distribution. The average pore size estimated was 44.8 µm, with a pore size distribution (Fig. 1D) that ranges mainly between 30 µm and 80 µm.
The scaffolds were also analyzed through pycnometry. Table 1 shows the porosity obtained and our structures are characterized by an ideal overall porosity for cell culture [44] .

Table 1: apparent volume, measured volume and porosity

Total apparent volume [cc]	2.448
Real volume measured [cc]	0.154
Overall porosity %	93.7 %

4.2 3D growth curves and morphological analysis of cells

MDA-MB-231 growth curve had already been shown in previous work [32]. The data obtained through the MTS assay, performed in triplicate after 1, 5, 10 and 14 days, allowed us to construct 3D growth curves shown in Fig.2A for MCF-7 and MCF-7R cell lines.

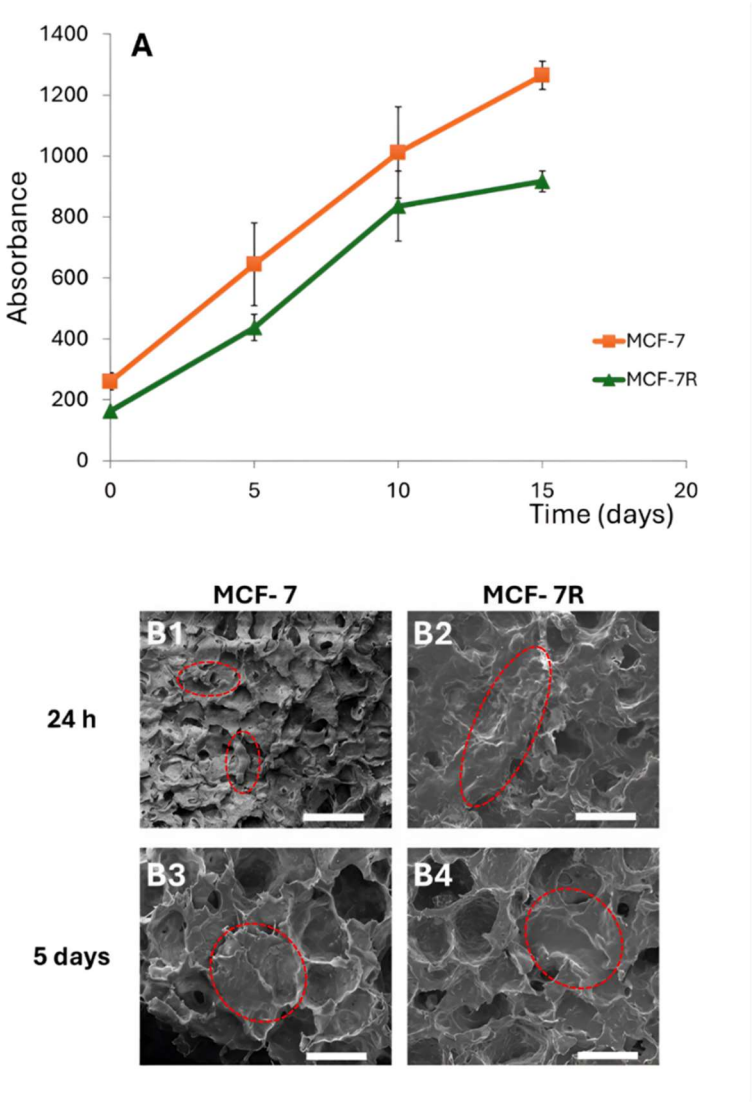

Figure 2: A) absorbance values from MTS assay for MCF-7 and MCF-7R at 1,5,10 and 14 days, N=3 replicates were used B1) SEM micrograph of MCF-7 cells at 24 h magnification 600x scale bar 100 µm. B2) SEM micrograph of MCF-7R cells at 24 h magnification 600x scale bar 100 µm. B3) SEM micrograph. of MCF-7 cells at 5 days magnification 600x scale bar 100 µm B4) SEM micrograph of MCF-7R cells at 5days magnification 600x scale bar 100 µm

Both curves show that cells can proliferate on the scaffold over time, as previously observed for the MDA-MB-231 cell line[32]. Furthermore, Figs 2 (B1-B4) show how both cell lines after 5 days can create a compact layer on the polymer matrix. For that reasons 5 days were chosen as starting time for doxorubicin treatment.

4.3 Breast cancer cells acquired chemoresistance in 3D culture

A live/dead assay was performed to assess cells' health prior to treatment (at 1 and 5 days of culture). Live/dead staining indicated that most cells survived and colonized the scaffold for 5 days; moreover, not only they adhered to the surface but were also able to migrate into matrix.

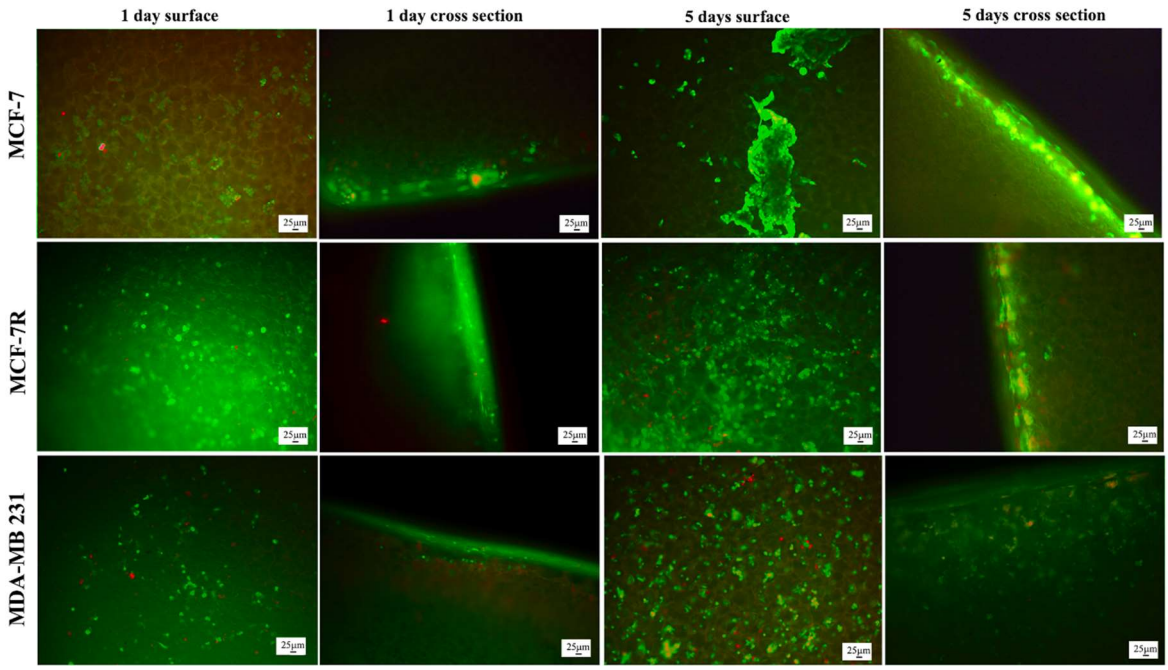

Figure 3: live/dead assay carried out on MDA-MB-231, MCF7 and MCF7-R cells grown in the scaffold for 1 and 5 days, on both surface and cross section.

Similar behavior was observed for all cell lines. Specifically, an increase in cell density could be observed after 5 days compared to 1 day of culturing. Most cells attached to the outer surface, but several cells can also be observed in the inner scaffold regions. To examine the inner regions, the scaffolds were cut with a blade before capturing microscopic images. This process resulted in the death of some cells, which were subsequently stained red.

The cytotoxicity of doxorubicin was evaluated in the three BC cell lines seeded on PLLA scaffold, by MTS assay. The graphs in Fig. 3A1, highlights a noticeable difference in the MDA-MB 231 cell line cultivated in 3D and in 2D: an increasing drug concentration was necessary in the treated 3D system to reach the IC_{50} that rises from 54.5 ng/ml in 2D to 445 ng/ml in 3D.

Regarding the MCF-7 cell line, Fig. A2 shows a very similar trend, with an IC_{50} of 0.75 μg/ml in 2D that rises to 7.45 μg/ml in 3D culture.
Cellular morphology undergoes significant alteration before and after reaching the IC_{50} threshold. MDA-MB-231 cells lose their typical clustered structure (Fig. B1-2). Regarding the MCF-7 cells, from Fig. B3-4 it can be noticed that the original layer appears to be disrupted after a doxorubicin treatment at a concentration higher than the IC_{50} value.

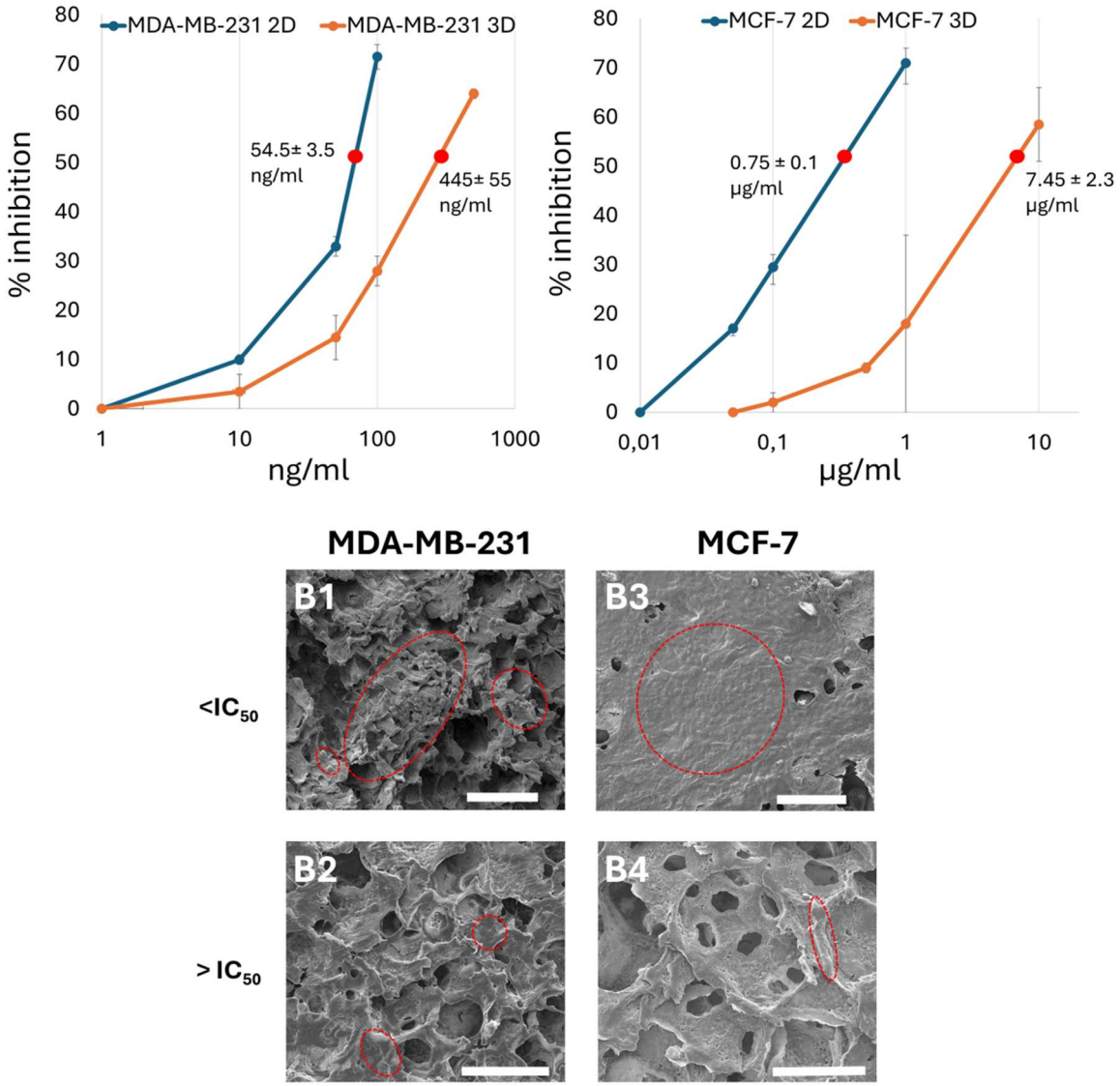

Figure 4: A1) % of growth inhibition from MTS assay for MDA-MB-231 cultivated in 2D (blue) and 3D (orange) for different doxorubicin concentrations, IC50 values are shown in both curves as red dots N=3 replicates were used.; A2) % of growth inhibition from MTS assay for MCF-7 cultivated in 2D (blue) and 3D (orange) for different doxorubicin concentrations, IC50 values are shown in both curves as red dots . N=3 replicates were used B1) SEM micrographs on healthy MDA-MB-231 cells grown in 3D, scale bar 100 µm magnification 600x, B2) SEM micrographs on MDA-MB-231 cells grown in 3D and treated with a doxorubicin concentration higher then IC_{50} value, scale bar 100µm magnification 800x; B3)SEM micrographs on healthy MCF-7 cells grown in 3D scale bar 100 µm magnification 600x; B4) SEM micrographs on MCF-7 cells grown in 3D and treated with a doxorubicin concentration higher then IC_{50} value, scale bar 100µm magnification 800x;

A very different behavior was observed for MCF-7R cell line. Firstly, in 2D cultures the IC_{50} value increases from 0.75 to 39 µg/ml with respect to the corresponding sensitive line. Going to 3D cultures, after 3 days from the treatment, the growth inhibition doesn't even reach the IC_{50} value (as witnessed by the orange dashed line in Fig. 4), despite the high concentrations tested (about 200 µg/ml).

A significantly longer exposure time (6 days) was necessary to reach a detectable IC_{50} value equal to 165 µg/ml. These data suggest that MCF-7R cells, grown in 3D, acquire a stronger

chemoresistance with respect to sensible line, leading one to suppose that they assume a spatial conformation that closely resembles the *in vivo* state.

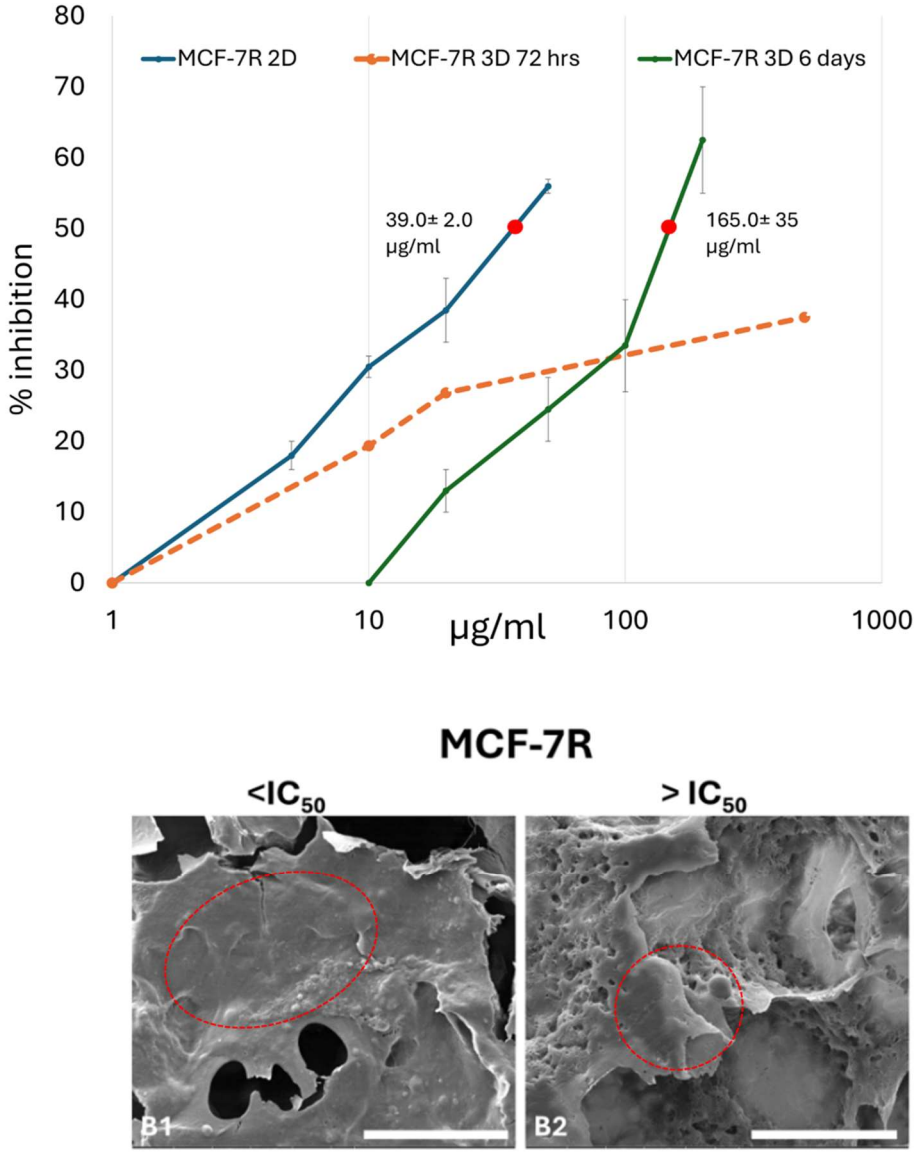

Figure 5: A) MCF-7R cells growth inhibition % after being treated with doxorubicin in 2D (blue) in 3D for 3 days (dashed orange) and in 3D for 6 days (grey) N=3 replicates were used ; B1) SEM micrographs on healthy MCF-7R cells grown in 3D, scale bar 40 µm magnification 2400x, B2) SEM micrographs on MCF-7R cells grown in 3D and treated with a doxorubicin concentration higher then IC_{50} value, scale bar 40µm magnification 2400x

Also, in this case different cells morphologies can be noticed when the cells are treated with a higher or lower concentration respect to the IC_{50} value. MCF-7R cells lose their typical epithelial behavior (Fig. B1), and as shown in Fig. B2 the original layer appears to be disrupted.

4.4 Is 3D culture chemoresistance associated with increased drug efflux?

P-glycoprotein (P-gp) efflux pump expression was analyzed at both transcriptional and protein level to evaluate if the penetration of doxorubicin was inhibited in 3D cultures by its overexpression. The doxorubicin sensitive line (MCF-7 cells) was chosen as control for this investigation as it lacks expression of P-gp. Figure 5 A clearly shows a notable increase in P-gp mRNA levels in the 3D culture, compared to that of the same 2D cells. However, these levels are clearly modest if compared to those of P-gp of the resistant 2D cell line (MCF-7R) characterized by a significant relative overexpression of the efflux pump (Figure 5 B). These results demonstrate that MCF-7 cells express high levels of P-gp mRNA when they grow in 3D, whereas they don't express it in 2D monolayers. However, this is not reflected in increased protein expression (too low to be shown).

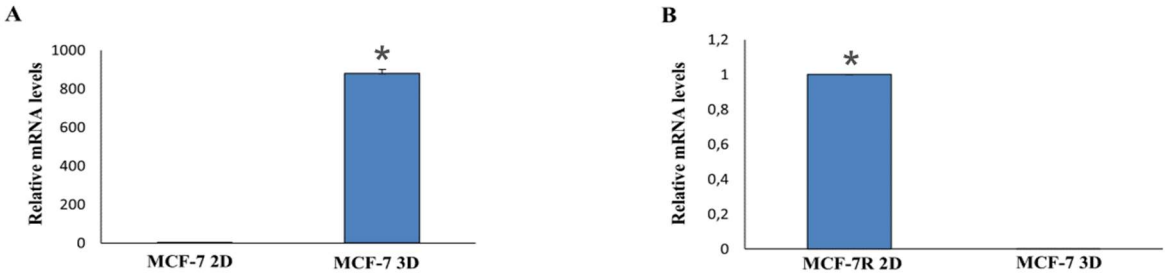

Figure 6: ***Expression of P-glycoprotein in 3D MCF-7 cell line by qRT-PCR****. A. Evaluation of P-gp mRNA expression levels in 3D MCF-7 cell line compared to those of the same 2D cell line. B. Evaluation of P-gp mRNA expression levels in 3D MCF-7 cell line compared to those of the MCF-7R cell line. For each condition, N=3 technical replicates were used. Data are expressed as mean ± standard error of two experiments. * = p<0.01*

5 Discussion

In recent years the discussion on the use of animals for pre-clinical testing has involved the entire scientific community which has looked for alternative tests to evaluate drug efficacy *in vitro*. In fact, in the USA a law allowing the FDA not to require animal models for the authorization of new drugs has already been approved [45]. On the other hand, it is known that 2D monolayer cultures are unsuitable for the study of anti-tumor molecules.
Since drug resistance in cancer cells challenges modern oncology, the exploration of innovative therapeutic strategies becomes necessary. Recent studies have highlighted the importance of understanding the molecular mechanism behind drug resistance, including genetic mutations, efflux pumps, altered signaling pathways and microenvironmental influences. Research aims to enhance the success of cancer treatments and increase patient survival rate. With this study we demonstrate that 3D scaffold-based models are able to provide a tumor microenvironment that better mimic the *in vivo* conditions offering a cost effective, scalable, and more ethical alternative for preclinical research [46], [47].

In this paper, we show the results by 3D cultures obtained with PLLA scaffolds. On these supports, we seeded three different breast cancer cell lines: triple negative breast cancer, MDA-MB-231, MCF-7 and its multidrug resistance variant, MCF-7R. The obtained data

showed that the scaffolds seem to produce a microenvironment for tumor cell growth *in vitro* that closely mimics *in vivo* conditions. The results align with previous studies that utilized devices for 3D growth of the same cell lines, showing consistent findings in terms of growth and morphology [48], [49].

As a matter of fact, for MDA-MB-231 and MCF-7 cells the IC_{50} values increases of about one order of magnitude when compared to 2D cultures. In the case of MCF7-R cell line, a longer exposure time (6 days) is needed to obtain an IC_{50}. The findings are consistent with earlier studies regarding chemotherapeutic drugs such as doxorubicin [50], [51].

It is possible to hypothesize that genotypic/phenotypic changes occur in cells growing in 3D models; such changes become more evident for cells characterized by multidrug resistance. This hypothesis is supported by data in the literature which indicate how 3D growth induces alterations in the cell cycle and variations in gene expression and in the levels of some proteins, implicated in the increase in aggression and in the development of the resistant phenotype [52]. In agreement with this hypothesis, our data indicate an increase in P-gp mRNA expression levels in MCF-7 cells grown in 3D, compared to the 2D model, demonstrating that the 3D environment of the scaffold favors the development of a resistant phenotype, thus supporting the higher concentration of doxorubicin needed to reach the IC_{50}. 3D environment alters probably in a limited and transient manner the expression of the P-gp, but only at transcriptional level in sensitive cells. Conversely, MDR cellular variant, not only exhibits higher levels of mRNA, but is also characterized by an overexpression of the protein.
Furthermore, data in the literature indicate that various cytoskeleton modifications are also associated with MDR phenotype and have been used as prognostic factors [53]. In this regard ongoing research of the authors shows that the growth of sensitive MCF-7 cells on the scaffold promotes the expression of vimentin, which is normally not expressed in such cells under 2D conditions. Vimentin plays a fundamental role in the ability of cells to invade the surrounding matrix, inducing the formation of metastases.
Overall, the presented data strengthens the hypothesis that the 3D growth onto the employed porous scaffolds favors the development of the resistant phenotype, indicating them as an excellent support for the study of this phenomenon.

6 Conclusions

Understanding MDR is very crucial in cancer research and novel advanced 3D models are necessary to study tumor microenvironment. This study highlights the potential of PLLA porous scaffolds produced by TIPS as perfect candidate to accomplish this objective, particularly in demonstrating significant differences in drug response and cellular behavior when compared to traditional 2D cultures. In fact, IC_{50} values for doxorubicin are markedly higher in 3D indicating an increasing resistance. Specifically for MDA-MB-231 this value rises from 54.5 ng/ml in 2D to 445 ng/ml in 3D; for MCF-7 cell line the IC_{50} of 0.75 μg/ml in 2D increases to 7.45 μg/ml in 3D culture; the MDR line MCF-7R demonstrates this trend even more pronounced with a doubled treatment time that was necessary to reach the IC_{50} equal to 165 μg/ml compared to 39 μg/ml in 2D. SEM micrographs reveal complex cellular architectures, cell clusters typical of MDA-MB-231 and compact layer for the MCF-7 sensible and resistant, that look like disrupted upon treatment with concentration higher than their respective IC_{50}. We investigated the molecular mechanism of resistance by

comparing P-gp mRNA expression in 2D and 3D MCF-7 cells and we showed that 3D cultures express higher levels respect to 2D although this did not translate into a corresponding increase in protein levels. This suggests a transcriptional but not translational response to the 3D environment, in fact the MCF-7R exhibits much higher levels of both mRNA and protein indicating that 3D microenvironment may induce a temporary and limited increase in P-gp expression in sensitive cells but not comparable to the MDR variants. In conclusion our study demonstrates that PLLA scaffold via TIPS offer a robust 3D system that enhance breast cancer understanding. This approach has the potential to bridge the gap between traditional monolayer culture and animal models leading to more effective and personalized treatment. Future perspective should include deeper investigation into molecular mechanism behind the observed drug resistance and further evaluation of PLLA 3D models potential for preclinical drug testing and development.

7 References

[1] B. Smolarz, A. Zadrożna Nowak, and H. Romanowicz, "Breast Cancer—Epidemiology, Classification, Pathogenesis and Treatment (Review of Literature)," May 01, 2022, *MDPI*. doi: 10.3390/cancers14102569.

[2] M. Arnold *et al.*, "Current and future burden of breast cancer: Global statistics for 2020 and 2040," *Breast*, vol. 66, pp. 15–23, Dec. 2022, doi: 10.1016/j.breast.2022.08.010.

[3] S. Nardin *et al.*, "Breast Cancer Survivorship, Quality of Life, and Late Toxicities," Jun. 16, 2020, *Frontiers Media S.A.* doi: 10.3389/fonc.2020.00864.

[4] Z. Gu, Q. Wu, B. Shang, K. Zhang, and W. Zhang, "Organoid co-culture models of the tumor microenvironment promote precision medicine," 2023, *John Wiley and Sons Inc*. doi: 10.1002/cai2.101.

[5] P. Poma *et al.*, "The antitumor activities of curcumin and of its isoxazole analogue are not affected by multiple gene expression changes in an MDR model of the MCF-7 breast cancer cell line: analysis of the possible molecular basis," *Int J Mol Med*, vol. 20, no. 3, pp. 329–335, 2007.

[6] M. Notarbartolo, M. Cervello, P. Poma, L. Dusonchet, M. Meli, and N. D'Alessandro, "Expression of the IAPs in multidrug resistant tumor cells," 2004.

[7] P. Poma, M. Labbozzetta, and M. Notarbartolo, "Patterns of Innate or Acquired Resistance to Anticancer Drugs: Our Experience to Overcome It," *Oncogenesis*, vol. 26, no. 2, pp. 27–37, 2021, [Online]. Available: www.begellhouse.com

[8] M. Bucci-Muñoz, A. M. Gola, J. P. Rigalli, M. P. Ceballos, and M. L. Ruiz, "Extracellular Vesicles and Cancer Multidrug Resistance: Undesirable Intercellular Messengers?," Aug. 01, 2023, *Multidisciplinary Digital Publishing Institute (MDPI)*. doi: 10.3390/life13081633.

[9] D. Manhas *et al.*, “Rottlerin promotes anti-metastatic events by ameliorating pharmacological parameters of paclitaxel: An in-vivo investigation in the orthotopic mouse model of breast cancer,” *Chem Biol Interact*, vol. 366, Oct. 2022, doi: 10.1016/j.cbi.2022.110109.

[10] L. Côrte-Real *et al.*, “Biotinylated Polymer-Ruthenium Conjugates: In Vitro and In Vivo Studies in a Triple-Negative Breast Cancer Model,” *Pharmaceutics*, vol. 14, no. 7, Jul. 2022, doi: 10.3390/pharmaceutics14071388.

[11] O. J. Egwom, M. Hassan, J. J. Tanimu, M. Hamada, and O. M. Ogar, “An LDA–SVM Machine Learning Model for Breast Cancer Classification †,” *BioMedInformatics*, vol. 2, no. 3, pp. 345–358, Sep. 2022, doi: 10.3390/biomedinformatics2030022.

[12] P. Mondal, K. L. Bailey, S. B. Cartwright, V. Band, and M. A. Carlson, “Large Animal Models of Breast Cancer,” Feb. 04, 2022, *Frontiers Media S.A.* doi: 10.3389/fonc.2022.788038.

[13] A. Moran-Alvarez, P. Gonzalez-Menendez, J. C. Mayo, and R. M. Sainz, “Reflections on the Biology of Cell Culture Models: Living on the Edge of Oxidative Metabolism in Cancer Cells,” Feb. 01, 2023, *MDPI*. doi: 10.3390/ijms24032717.

[14] E. M. Tosca, D. Ronchi, D. Facciolo, and P. Magni, “Replacement, Reduction, and Refinement of Animal Experiments in Anticancer Drug Development: The Contribution of 3D In Vitro Cancer Models in the Drug Efficacy Assessment,” Apr. 01, 2023, *MDPI*. doi: 10.3390/biomedicines11041058.

[15] G. Arnason, “The Emergence and Development of Animal Research Ethics: A Review with a Focus on Nonhuman Primates,” *Sci Eng Ethics*, vol. 26, no. 4, pp. 2277–2293, Aug. 2020, doi: 10.1007/s11948-020-00219-z.

[16] M. Lakshmanan, D. G. Shewade, and G. M. Raj, *Introduction to Basics of Pharmacology and Toxicology: Volume 3: Experimental Pharmacology: Research Methodology and Biostatistics*, vol. 3. Springer Nature, 2022. doi: 10.1007/978-981-19-5343-9.

[17] A. Vashishat, P. Patel, G. Das Gupta, and B. Das Kurmi, “Alternatives of Animal Models for Biomedical Research: a Comprehensive Review of Modern Approaches,” *Stem Cell Rev Rep*, 2024, doi: 10.1007/s12015-024-10701-x.

[18] P. Mukherjee, S. Roy, D. Ghosh, and S. K. Nandi, “Role of animal models in biomedical research: a review,” Dec. 01, 2022, *BioMed Central Ltd*. doi: 10.1186/s42826-022-00128-1.

[19] H. Kolahi Azar *et al.*, “The progressive trend of modeling and drug screening systems of breast cancer bone metastasis,” Dec. 01, 2024, *BioMed Central Ltd*. doi: 10.1186/s13036-024-00408-5.

[20] J. P. Mather, “Concise review: Cancer stem cells: In vitro models,” Feb. 2012. doi: 10.1002/stem.774.

[21] M. Kapałczyńska *et al.*, “2D and 3D cell cultures – a comparison of different types of cancer cell cultures,” *Archives of Medical Science*, vol. 14, no. 4, pp. 910–919, 2018, doi: 10.5114/aoms.2016.63743.

[22] F. Antonelli, “3D Cell Models in Radiobiology: Improving the Predictive Value of In Vitro Research,” Jul. 01, 2023, *Multidisciplinary Digital Publishing Institute (MDPI)*. doi: 10.3390/ijms241310620.

[23] N. S. Wind and I. Holen, “ Multidrug Resistance in Breast Cancer: From In Vitro Models to Clinical Studies ,” *Int J Breast Cancer*, vol. 2011, pp. 1–12, 2011, doi: 10.4061/2011/967419.

[24] C. Jubelin *et al.*, “Three-dimensional in vitro culture models in oncology research,” Dec. 01, 2022, *BioMed Central Ltd*. doi: 10.1186/s13578-022-00887-3.

[25] J. Bin Kim, R. Stein, and M. J. O’hare, “Three-dimensional in vitro tissue culture models of breast cancer-a review,” 2004.

[26] C. Jubelin *et al.*, “Three-dimensional in vitro culture models in oncology research,” Dec. 01, 2022, *BioMed Central Ltd*. doi: 10.1186/s13578-022-00887-3.

[27] P. Mu *et al.*, “Newly developed 3D in vitro models to study tumor–immune interaction,” Dec. 01, 2023, *BioMed Central Ltd*. doi: 10.1186/s13046-023-02653-w.

[28] D. M. Engrácia, C. I. G. Pinto, and F. Mendes, “Cancer 3D Models for Metallodrug Preclinical Testing,” Aug. 01, 2023, *Multidisciplinary Digital Publishing Institute (MDPI)*. doi: 10.3390/ijms241511915.

[29] D. Caballero *et al.*, “Forecast cancer: the importance of biomimetic 3D in vitro models in cancer drug testing/discovery and therapy,” *In vitro models*, vol. 1, no. 2, pp. 119–123, Apr. 2022, doi: 10.1007/s44164-022-00014-z.

[30] A. Ahmad, Ed., *Breast Cancer Metastasis and Drug Resistance*, Second., vol. 1152. in Advances in Experimental Medicine and Biology, vol. 1152. Mobile, AL, USA: Springer International Publishing, 2019. doi: 10.1007/978-3-030-20301-6.

[31] D. Sztankovics *et al.*, “3D bioprinting and the revolution in experimental cancer model systems—A review of developing new models and experiences with in vitro 3D bioprinted breast cancer tissue-mimetic structures,” *Pathology and Oncology Research*, vol. 29, Feb. 2023, doi: 10.3389/pore.2023.1610996.

[32] M. E. Lombardo *et al.*, “PLLA scaffolds with controlled architecture as potential microenvironment for in vitro tumor model,” *Tissue Cell*, vol. 58, 2019, doi: 10.1016/j.tice.2019.04.004.

[33] K. Sharma, S. Dey, R. Karmakar, and A. K. Rengan, “A comprehensive review of 3D cancer models for drug screening and translational research,” 2023, *John Wiley and Sons Inc*. doi: 10.1002/cai2.102.

[34] H. T.-L. Nguyen, S. T. Nguyen, and P. Van Pham, “Concise Review: 3D cell culture systems for anticancer drug screening,” *Biomedical Research and Therapy*, vol. 3, no. 5, Jun. 2016, doi: 10.7603/s40730-016-0022-8.

[35] R. Li, Y. H. Ting, S. H. Youssef, Y. Song, and S. Garg, “Three-dimensional printing for cancer applications: Research landscape and technologies,” Aug. 01, 2021, *MDPI*. doi: 10.3390/ph14080787.

[36] H. Bhuskute, P. Shende, and B. Prabhakar, “3D Printed Personalized Medicine for Cancer: Applications for Betterment of Diagnosis, Prognosis and Treatment,” Jan. 01, 2022, *Springer Science and Business Media Deutschland GmbH*. doi: 10.1208/s12249-021-02153-0.

[37] A. J. R. Barcena, K. Dhal, P. Patel, P. Ravi, S. Kundu, and K. Tappa, “Current Biomedical Applications of 3D-Printed Hydrogels,” Jan. 01, 2024, *Multidisciplinary Digital Publishing Institute (MDPI)*. doi: 10.3390/gels10010008.

[38] E. Prince *et al.*, “Biomimetic hydrogel supports initiation and growth of patient-derived breast tumor organoids,” *Nat Commun*, vol. 13, no. 1, Dec. 2022, doi: 10.1038/s41467-022-28788-6.

[39] R. Schmid *et al.*, “Comparison of hydrogels for the development of well-defined 3d cancer models of breast cancer and melanoma,” *Cancers (Basel)*, vol. 12, no. 8, pp. 1–21, Aug. 2020, doi: 10.3390/cancers12082320.

[40] H. Xin and S. Naficy, “Drug Delivery Based on Stimuli-Responsive Injectable Hydrogels for Breast Cancer Therapy: A Review,” Jan. 01, 2022, *MDPI*. doi: 10.3390/gels8010045.

[41] A. J. R. Barcena, K. Dhal, P. Patel, P. Ravi, S. Kundu, and K. Tappa, “Current Biomedical Applications of 3D-Printed Hydrogels,” Jan. 01, 2024, *Multidisciplinary Digital Publishing Institute (MDPI)*. doi: 10.3390/gels10010008.

[42] F. Carfì Pavia, V. La Carrubba, S. Piccarolo, and V. Brucato, “Polymeric scaffolds prepared via thermally induced phase separation: Tuning of structure and morphology,” *J Biomed Mater Res A*, vol. 86, no. 2, 2008, doi: 10.1002/jbm.a.31621.

[43] Arash Rabbani, “SEM Image Porosity and Pore Size,” https://it.mathworks.com/matlabcentral/fileexchange/70245-sem-image-porosity-and-pore-size.

[44] Q. L. Loh and C. Choong, “Three-dimensional scaffolds for tissue engineering applications: Role of porosity and pore size,” Dec. 01, 2013. doi: 10.1089/ten.teb.2012.0437.

[45] M. Wadman, “FDA no longer has to require animal testing for new drugs,” *Science (1979)*, vol. 379, no. 6628, pp. 127–128, Jan. 2023, doi: 10.1126/science.adg6276.

[46] P. Garg, J. Malhotra, P. Kulkarni, D. Horne, R. Salgia, and S. S. Singhal, “Emerging Therapeutic Strategies to Overcome Drug Resistance in Cancer Cells,” *Cancers (Basel)*, vol. 16, no. 13, p. 2478, Jul. 2024, doi: 10.3390/cancers16132478.

[47] U. L. Tratar, S. Horvat, and M. Cemazar, “Transgenic mouse models in cancer research,” Jul. 20, 2018, *Frontiers Media S.A.* doi: 10.3389/fonc.2018.00268.

[48] C. Liverani *et al.*, “Investigating the Mechanobiology of Cancer Cell–ECM Interaction Through Collagen-Based 3D Scaffolds,” *Cell Mol Bioeng*, vol. 10, no. 3, pp. 223–234, Jun. 2017, doi: 10.1007/s12195-017-0483-x.

[49] C. Liverani *et al.*, “A biomimetic 3D model of hypoxia-driven cancer progression,” *Sci Rep*, vol. 9, no. 1, Dec. 2019, doi: 10.1038/s41598-019-48701-4.

[50] M. Alwahsh, A. Al-Doridee, S. Jasim, O. Awwad, R. Hergenröder, and L. Hamadneh, “Cytotoxic and molecular differences of anticancer agents on 2D and 3D cell culture,” *Mol Biol Rep*, vol. 51, no. 1, Dec. 2024, doi: 10.1007/s11033-024-09669-1.

[51] C. Jaiswal and B. B. Mandal, “A 3D In Vitro Triculture Hybrid Model Recapitulating Tumor Stromal Interaction of Triple-Negative Breast Cancer as a High Throughput Anticancer Drug Screening Platform,” *Adv Ther (Weinh)*, vol. 7, no. 5, May 2024, doi: 10.1002/adtp.202300450.

[52] Y. Ding *et al.*, “Three-dimensional tissue culture model of human breast cancer for the evaluation of multidrug resistance,” *J Tissue Eng Regen Med*, vol. 12, no. 9, pp. 1959–1971, Sep. 2018, doi: 10.1002/term.2729.

[53] F. Bichat, R. Mouawad, G. Solis-Recendez, D. Khayat, and G. Bastian, “Cytoskeleton alteration in MCF7R cells, a multidrug resistant human breast cancer cell line,” *Anticancer Res*, vol. 17, no. 5A, p. 3393—3401, 1997, [Online]. Available: http://europepmc.org/abstract/MED/9413178